https://doi.org/10.5194/egusphere-2026-995
Preprint. Discussion started: 6 March 2026

Biogeochemical controls on nutrient fluxes in small tropical mountainous river basins: Mechanisms for P-limitation and Si-rich conditions

Upendra Badimela[1,2*], Kiran Kumar Reddy[1], Jesuraja Kamaraj[1], Ciba Manohar[1], Vidya Suresh[1], Vinnetha Perumbully[1], Anoop Krishnan[1]

[1]Environmental Hydrology Group, National Centre for Earth Science Studies (NCESS), Thiruvananthapuram-695011, India.

[2]Department of Applied Chemistry, Cochin University of Science and Technology (CUSAT), Kochi-682022, India.

*Corresponding author: E-mail address: upendra.b@ncess.gov.in Tel.: +91-0471-251-1700

https://doi.org/10.5194/egusphere-2026-995
Preprint. Discussion started: 6 March 2026

Abstract

Small scale mountainous rivers with their quick flowing mechanisms provide a clear understanding on the nutrient flux dynamics in assessing their role in biogeochemical cycles and coastal nutrient budgets. The present study examines the spatio-temporal variability of dissolved inorganic nutrients in the Karamana River Basin (KRB) and Vamanapuram River Basin (VRB), flowing through Western Ghats, which emphasis the hydro geochemistry, segment-wise nutrient fluxes, and their biogeochemical cycle implications. The results reveal marked spatio-temporal variability in nutrient fluxes similar to the hydrochemistry, with higher fluxes generally recorded during the MON due to enhanced runoff and weathering. The segment-wise average fluxes of DIN, DIP, and DSi in the KRB were estimated at 6.84, 0.05, and 127.25 kg ha^{-1} yr^{-1}, respectively. In comparison, the corresponding values for the VRB were 9.44, 0.07, and 81.66 kg ha^{-1} yr^{-1}, respectively. A clear indication of low concentration conditions in the upstream followed by slight enrichment in the mid and downstream regions further highlight pristine environment and the role of land use and anthropogenic influence, respectively. The stagnant conditions after reaching the downstream regions with favorable tropical climate conditions promoting the consumption of nutrients through in-situ production. The DSi flux of VRB (127.25 kg ha^{-1} yr^{-1}) is comparable to that of large global rivers such as the Amazon (108.6 kg ha^{-1} yr^{-1}) and Mississippi (118.21 kg ha^{-1} yr^{-1}), further supports the claim of intense chemical weathering derived silica-rich conditions. Overall, the study highlights the critical role of climate and topography in regulating nutrient fluxes and confirms that nutrient inputs from these small-scale mountainous rivers have a relatively limited influence on coastal eutrophication in the receiving zones.

Keywords: Biogeochemical cycles; Chemical weathering; Dissolved inorganic nutrients, P-limitation; Tropical-mountainous rivers.

https://doi.org/10.5194/egusphere-2026-995
Preprint. Discussion started: 6 March 2026

1. Introduction

A clear understanding on the nutrient fluxes from rivers to receiving coastal zones is governed by several factors including the climate (Meybeck, 1982). Such understanding is complex for the large-scale rivers and in the regions evidencing the rapid expansion of urbanization, industrialization agricultural, and domestic sewage sources into local rivers and finally reaching coastal waters (Meybeck, 1982; Tong et al., 2015; Ni et al., 2018; Aniebone et al., 2024; Rangel-Buitrago et al., 2024). The way these nutrients are transported and transformed within the river can vary widely, depending on both short-term changes in water flow and long-term shifts in land use patterns and population growth (Basu et al., 2010). These fluctuations can shift which nutrients become limiting for ecosystem productivity, potentially reshaping the structure and functioning of aquatic environments. One major factor influencing these nutrient fluxes is river length (or overall size). Large river systems that originate in hilly regions typically follow topographic gradients until they reach coastal mixing zones. Such rivers have long flow paths, steep upstream gradients, and a relatively small proportion of upstream area (<10%), while much of their drainage basin is exposed to anthropogenic activities. In contrast, small mountainous rivers flow rapidly due to steep terrain and have a more balanced distribution of pristine (hilly) and human-impacted zones. Consequently, these two types of fluvial systems exhibit distinct hydrological, biogeochemical, and elemental flux transport characteristics including nutrients.

Among the macro nutrients, the dissolved inorganic nitrogen (N), phosphorus (P), and silica (DSi) are key nutrients that play a critical role of the primary productivity regulation in aquatic ecosystems (Meybeck, 1982; Li et al., 2007; Reddy et al., 2024). This problem is more intense in heavily populated regions, where the nutrient input into river systems is influenced by various interconnected factors like hydrological conditions (Alexander et al., 2008), land-based nutrient

https://doi.org/10.5194/egusphere-2026-995
Preprint. Discussion started: 6 March 2026

sources (Bouwman et al., 2009; Garnier et al., 2010; Reddy et al., 2024), and the natural in-situ processes stirring (Seitzinger et al., 2005; Reddy et al., 2021). These processes also affect nutrient transformation, retention, and removal during their downstream flow (Nie et al., 2018; Finkler et al., 2023). These processes ultimately lead to increased nutrient levels or the limitation of one or more nutrients (Conley et al., 2009; Turner et al., 2010; Wei et al., 2023; Reddy et al., 2024). It's also reported the limitation of individual nutrient and the excess input of other nutrient within the same river system is evidenced (Houser and Richardson, 2010; Reddy et al., 2024). Understanding the mechanisms that regulate these processes is essential for improving our knowledge of fluvial biogeochemistry and informing future restoration strategies.

Considering this, the current article is mainly focusing on two small-scale mountainous rivers with source to sink seasonal sampling. This study aims to (1) assess the seasonal and spatial variations in key hydrological parameters, including nutrient concentrations, across two small tropical mountainous rivers; (2) identify and compare the primary nutrient sources in the upstream, midstream, and downstream zones during three distinct seasons; and (3) investigate the processes governing the seasonal distribution and transport of nutrients across these three river segments.

2. Methods

2.1 Study area

The study area consists of small-scale tropical mountainous rivers, Karamana (KRB) and Vamanapuram river (VRB) basins, originating in the Western Ghats (WG) mountainous peaks (~1600 m; Fig. 1) and flowing towards the west and discharging to Arabian Sea. Each basin is divided into three equal parts to represent the upstream, mid and downstream processes (Fig. 1). The WG region receives annual rainfall of 3554 mm with a variability ranging from 490-5644 mm (Reddy et al., 2019). The current study basins received 2520 mm rainfall during the study period

https://doi.org/10.5194/egusphere-2026-995
Preprint. Discussion started: 6 March 2026

(Upendra et al., 2025). The climate of the region is categorized as tropical monsoon with four seasons i.e., pre-monsoon, SW monsoon, NE monsoon, and a post monsoon. Out of which contributions from monsoon is ~84% (Reddy et al., 2021). The region's mean temperature, based on atmospheric data from multiple sampling points during the study period, is approximately 29°C, with a range between 22°C and 32.5°C. Geologically, it lies within the Southern Granulite Terrain, predominantly composed of Archean crystalline rocks and Proterozoic metasupracrustals, including leptynites and khondalites (Fig. S1). The area also contains intrusions such as pegmatite veins, dolerite dykes, and quartz veins (Anu-Sha et al., 2024). In the coastal zone, Quaternary sediments and Warkalli beds are discontinuously overlaid on the crystalline basement (Padmalal, 1996; Varghese et al., 2016). The region supports diverse land use, including agriculture, plantations, forests, and urban settlements, with key crops such as spices, rice, rubber and coconut (Reddy et al., 2021; Fig. S2). Soil types, classified by the Food and Agriculture Organization, range from sandy loam to clay loam (Upendra et al., 2024).

https://doi.org/10.5194/egusphere-2026-995
Preprint. Discussion started: 6 March 2026

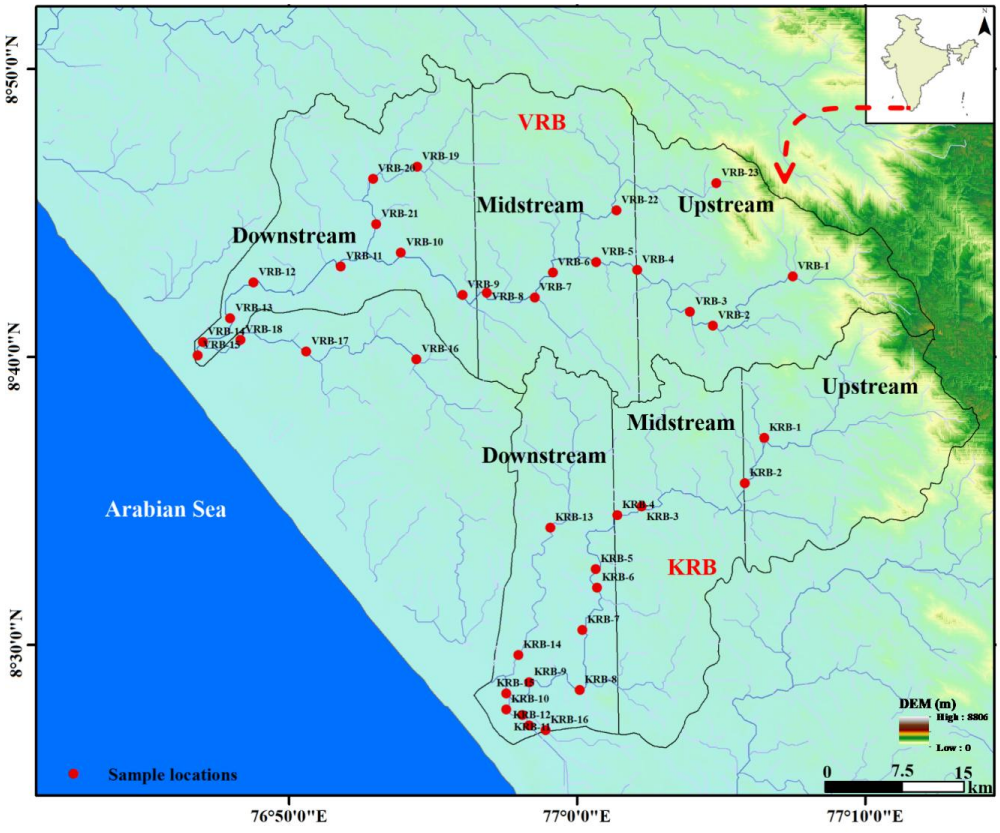

Fig. 1: Map showing the spatial extent of study basins, sampling locations and the source to sink topography.

2.2 Sample collection

Seasonal and source-to-sink sampling was conducted across the Pre-monsoon (March 2022), Monsoon (July 2022), and Post-monsoon (January 2023) periods, covering both the main stream and its principal tributaries of both the basin (Fig. 1). The samples were collected in precleaned 1L and 500 mL high-density polyethylene bottles for anion and cation from middle of the river course using locally hired boats, respectively. After collecting cation samples, 1-2 drops of 2 N nitric acid (HNO_3; Merck) was added immediately to preserve metal cations. All the samples were kept in

https://doi.org/10.5194/egusphere-2026-995
Preprint. Discussion started: 6 March 2026

portable car chillers (~4°C) during the sampling and subsequently stored at the clean chemistry laboratory refrigerators at the NCESS for hydro-geochemical analysis.

2.3 Analysis

Soon after collecting each sample, in-situ measurements for key parameters (pH, EC, and TDS) were measured using the multiparameter probe H1198, with reported accuracy of ±2 pH unit, ±1 µS/cm, and ±1 mg L^{-1}, respectively. In the clean laboratory, the samples were filtered using 0.45 µM membrane filters (Whatman), and subsequently the nutrient analysis was mainly carried out using the Continuous Flow Analyzer (Model: Skalar, San++). The CFA measures the inorganic elemental form of nutrients like NO_3-N, NO_2-N, PO_4-P, and SiO_4-Si. The current study reported the nutrient data i.e., NO_3^-+NO_2-N, PO_4^{3-}-P, and SiO_2-Si as DIN, DIP, and DSi. The methodological precision of the analysis was ≤1.5% for DIN (NO_3^- + NO_2^-), ≤1.5% for DIP (PO_4^{3-}), and ≤2.0% for DSi (H_2SiO_4), based on replicate standard and duplicate sample measurements. The NH_4^+ concentration was all the time below the detection limit and therefore excluded from the calculation of DIN. Further, the major cations ions were analysed using the ion chromatography (Dionex Aquion, Thermo). The precision for the mixed standard was ±2%. Finally, to ensure data consistency, a normalized inorganic charge balance was performed on the data using the following equation

$$NICB = [(Tz^+ - Tz^-)/(Tz^+ + Tz^-)] \times 100$$

Most of the samples from both the river basins showed a specific charge balance (NICB) within ±10%. The supporting data to calculate the flux, such as water discharge values, were recorded exclusively at the basin outlet, as in-situ measurements at individual sites were not feasible due to site-specific constraints, including accessibility issues, flow conditions, and safety concerns.

https://doi.org/10.5194/egusphere-2026-995
Preprint. Discussion started: 6 March 2026

2.3 Segment wise nutrient flux calculation

This study further estimated the nutrient flux of river basin by employing a segment-wise classification of the study area. This segment wise classification was employed to assess the impact of topographical and land-use over nutrient dynamics. Both river basins, KRB and VRB, were divided into three segments and estimated the area of both river basins using the python. The relative discharge approach of David et al. (2016), applicable to Kerala rivers (Upendra et al., 2025), is followed to derive discharge data. The same is used for the calculation of segment-wise nutrient load and nutrient yield using the following equations

Relative discharge, $Q\ (km^3\ km^{-2}\ yr^{-1}) = Q_m/A_m$

Discharge per Segment, $Q_s\ (km^3\ yr^{-1}) = A_s \times Q$

Nutrient load, $L_n\ (t\ yr^{-1}) = C \times Q_s \times 1000$

Nutrient Yield, $Y_n = L_n/A_s \times 10$

Q_m and Q_s are the discharge corresponding to the outlet and each segment expressed as $km^3 yr^{-1}$, while the A_m and A_s are the basin area in km^2; similarly, the L_n and Y_n are the nutrient load and yield, expressed in $t\ yr^{-1}$ and $kg\ ha^{-1}\ yr^{-1}$, respectively. Moreover, the concentration of ions is taken in $mg\ L^{-1}$.

2.4 Calculation of Coastal Eutrophication Potential Indicator (ICEP)

The study also tries to assess the ICEP, the potential quantity of non-siliceous algal biomass that may be produced in coastal waters because of an overabundance of nitrogen or phosphorus in comparison to silica input. It employs a conventional nutrient ratio for algae, specifically the Redfield molar ratio of C:N:P: Si set at 106:16:1:20, which indicates the balanced nutrient composition essential for algal growth (Garnier et al., 2010). To compare different rivers, ICEP values are adjusted according to the size of each river basin and are expressed as kilograms of

https://doi.org/10.5194/egusphere-2026-995
Preprint. Discussion started: 6 March 2026

carbon per square kilometer per day (kg C km^{-2} d^{-1}). When nitrogen is an excess nutrient, it's called N-ICEP; if phosphorus is in excess, it's called P-ICEP (Billen and Garnier, 2007), based on formulas (1) and (2).

$$\text{N-ICEP} = [N_{Flux}/(14\times16) - Si_{Flux}/(28\times20)] \times 10^6 \times 12$$

$$\text{P-ICEP} = [P_{Flux}/(1\times31) - Si_{Flux}/(28\times20)] \times 10^6 \times 12$$

Where N_{Flux}, P_{Flux}, and Si_{Flux} represent the average specific fluxes respectively, at the outlet of the river basin, measured in kg P km^{-2} d^{-1}, kg N km^{-2} d^{-1}, kg Si km^{-2} d^{-1}.

3. Results

3.1 Hydrogeochemical Characteristics

The Piper diagram of KRB and VRB showed that 64.71% of the total water samples of both the KRB and VRB are classified as Ca-Mg-HCO_3, followed by 19.61% as Na-K-Cl-SO_4, and 15.69% as mixed type water (Fig. 2**)**. However, when examining the individual water characteristics for both KRB and VRB, the trend varies slightly, as VRB exhibits a greater prevalence of mixed water characteristics following Ca-Mg-HCO_3 compared to KRB (Fig. S3). Spatially, water samples of KRB represents the same water types with percentages of 56.25%, 27.08%, and 16.67%, respectively. In contrast, the water characteristics percentages for VRB are 81.25%, 6.25%, and 25%, indicate the more dominance of Ca-Mg-HCO_3 type. Seasonally, during the MON season, approximately 99% of KRB water samples display the Ca-Mg-HCO_3 water type, with the Na-K-Cl-SO_4 water character being absent. In the PRM season, around 1% of samples show Na-K-Cl-SO_4 characteristics, with the highest percentage being in the Ca-Mg-HCO_3 type. Conversely, in the POM season, the prevalence of Ca-Mg-HCO_3 type water is lower compared to mixed type and Na-K-Cl-SO_4 waters, with the number of samples exhibiting this character being similar. In VRB,

https://doi.org/10.5194/egusphere-2026-995
Preprint. Discussion started: 6 March 2026

182 approximately 60% of total water samples across all seasons demonstrate Ca-Mg-HCO_3 type
183 characteristics, while the POM season does not present mixed type water, and the influence of Ca-
184 Mg-HCO_3 is predominant during this season.

185

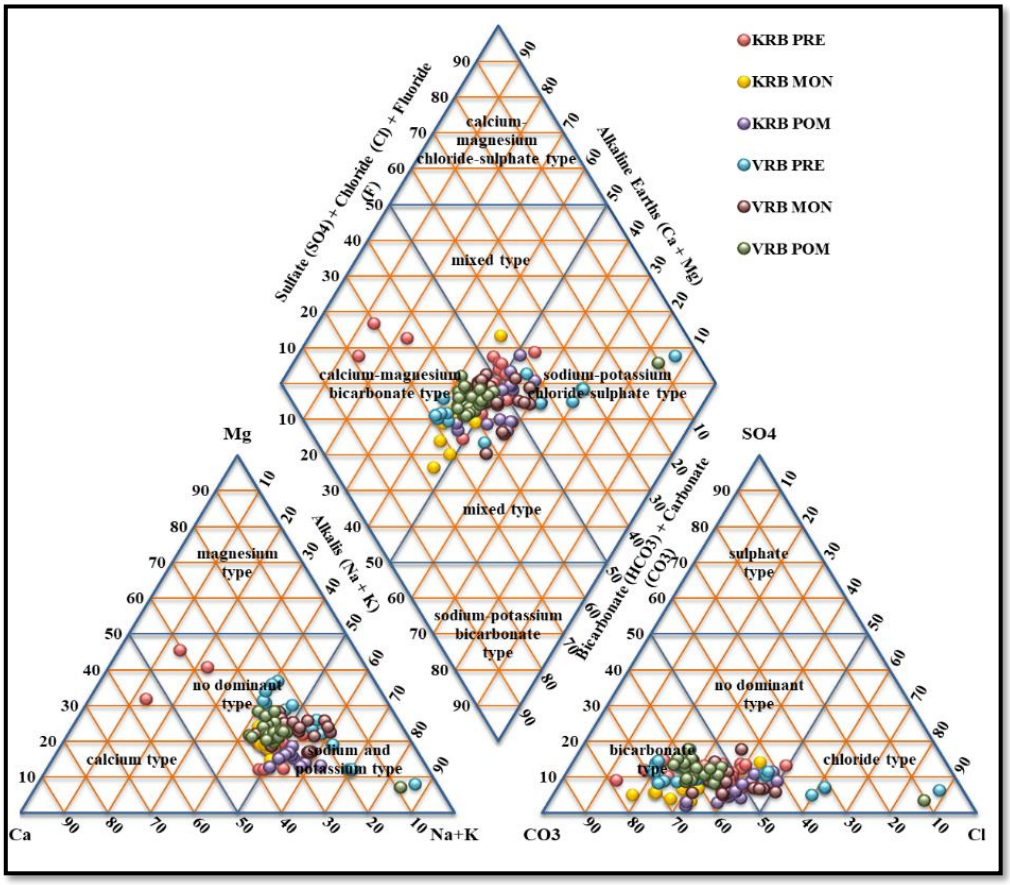

200

201 **Fig. 2:** Piper plot represents mixed type of water along with the post monsoon samples in Ca-
202 Mg-HCO3 and downstream samples in Na-K-Cl-SO4 zone for KRB and VRB.

203

204

205

https://doi.org/10.5194/egusphere-2026-995
Preprint. Discussion started: 6 March 2026

3.2 Hydrogeochemical Variations

The hydrochemistry of the KRB and VRB displayed distinct variations across all measured parameters. For instance, pH values ranged from 5.04 to 7.23, with a mean of 6.38 while VRB recorded a pH range of 6.6 to 8.2 and an average of 7.42, reflecting neutral to slightly alkaline. Spatially, the upstream regions showing acidic (5.04-6.18) and seasonally the MON season showing low pH values compared to PRM and POM. On the other hand, most of the major cations followed similar trend irrespective of seasons. Spatially, Ca^{2+}, Mg^{2+}, Na^{+}, and K^{+} and concentrations in KRB and VRB displayed consistent patterns in all the seasons (Fig. 3). The concentrations of all these cations were higher in KRB basin compared to VRB. Among the cations, the bicarbonate (HCO_3^{-}), a major species of dissolved inorganic carbon, displayed a significant source to sink variability where the downstream region witnessing two orders the concentrations in midstream region irrespective of season. Interestingly unlike the major cations, the HCO_3^{-} concentration was significantly lower in the upstream regions of both the basins (Fig. 4). These reported major ions and HCO_3^{-} concentrations are consistent with the earlier reports (Upendra et al., 2025) and sourced mainly through bed-rock and river water interaction (Fig. S4).

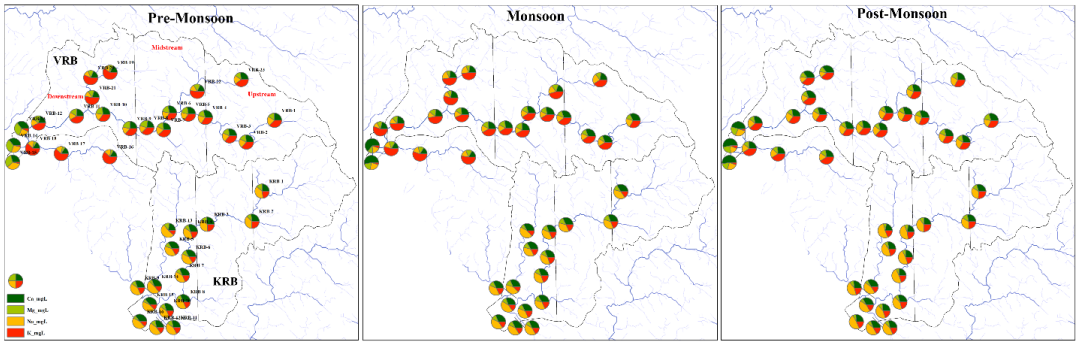

Fig. 3: Seasonal and spatial variability of selected major cations (Ca^{2+}, Mg^{2+}, Na^{+}, and K^{+}) across the two basins.

https://doi.org/10.5194/egusphere-2026-995
Preprint. Discussion started: 6 March 2026

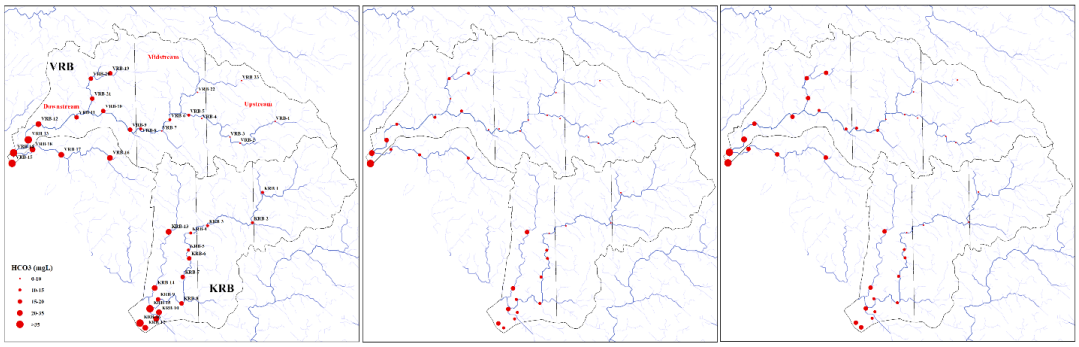

Fig. 4: Seasonal and spatial variability of the HCO_3^- concentration from both the basins.

3.3 Nutrient Concentrations

The nutrient concentration levels in the KRB display clear seasonal trends corresponding to the PRM, MON, and POM seasons (Fig. 4). Individually, DIN concentrations peaked during the PRM (Fig. 4b) season for KRB, averaging around 0.43 mg L^{-1}, followed by moderate levels in both the monsoon (0.26 mg L^{-1}) and post-monsoon (0.27 mg L^{-1}) seasons. Moreover, in POM season, most of the DIN concentration (i.e., ~25-75%) falls below the mean value, implying that a few high values (outliers) are pulling the mean upward, but most of the data exhibit lower values (Fig 4b). The elevated sample values are attributed to the presence of higher values recorded in the tributary river, especially at Jagathy (KRB-14) and the Kalady region (KRB-15). These areas are densely populated and include prime industrial zones within the Trivandrum district (Fig. S2). In VRB, the DIN values were marked high (1.94 mg L^{-1}) in the PRM season and low (0.13 mgL^{-1}) during the MON season (Fig. 4d). On the other hand, DIP levels extremely low compared to other nutrients in both rivers (Fig. 4d). In KRB, the highest value observed in the MON (4.46 µg L^{-1} season at the outlet of the basin while the lowest value observed in the PRM season at the upstream (0.21 µg L^{-1}) region. The seasonal range of DIP concentrations in KRB (Fig. 4b) showed mean values of 0.58 µg L^{-1} (PRM), 2.26 µgL^{-1} (MON), and 1.90 µgL^{-1} (POM). Comparing seasonally highest values

https://doi.org/10.5194/egusphere-2026-995
Preprint. Discussion started: 6 March 2026

were reported in the MON season and lowest in the PRM season. Unlike other parameters the DIP values were decreasing consistently downward suggesting a strong spatial heterogeneity, nutrient retention and flushing efficiency. Similarly, for VRB, the mean values of 4.04 µg L^{-1}, 8.73 µg L^{-1}, and 5.87 µg L^{-1} for PRM, MON, and POM, respectively. Irrespective of the season, the lowest DIP value was evidenced at the outlet of both the basins. These finding highlights distinct DIP behavior in small tropical rivers.

DSi concentrations were higher among the three nutrients and highest during the PRM in both the river basins (Fig. 4a). In the KRB, the DSi range and mean (Fig. 4a) show a highest value of 6.28 mg L^{-1} at the outlet during PRM and lowest (3.24 mg L^{-1}) during the MON season. In contrast to DIP concentrations, the Dsi concentrations displayed a gradual downstream increasing trend irrespective of season in both the basins. In the VRB, the reported values are higher than those in the KRB (Fig. 4c). The highest DSi concentration in VRB (8.02 mg L^{-1}) was measured during the PRM monsoon at the outlet and during the MON, values declined (~4.61 mg L^{-1}) due to the dilution from heavy rainfall and surface runoff, while POM concentrations (~7.98 mg L^{-1}) remained relatively moderate. Though the source to sink nutrient concentrations were unique from this study, however, the outlet concentrations are consistent with the recent findings (Reddy et al., 2024).

https://doi.org/10.5194/egusphere-2026-995
Preprint. Discussion started: 6 March 2026

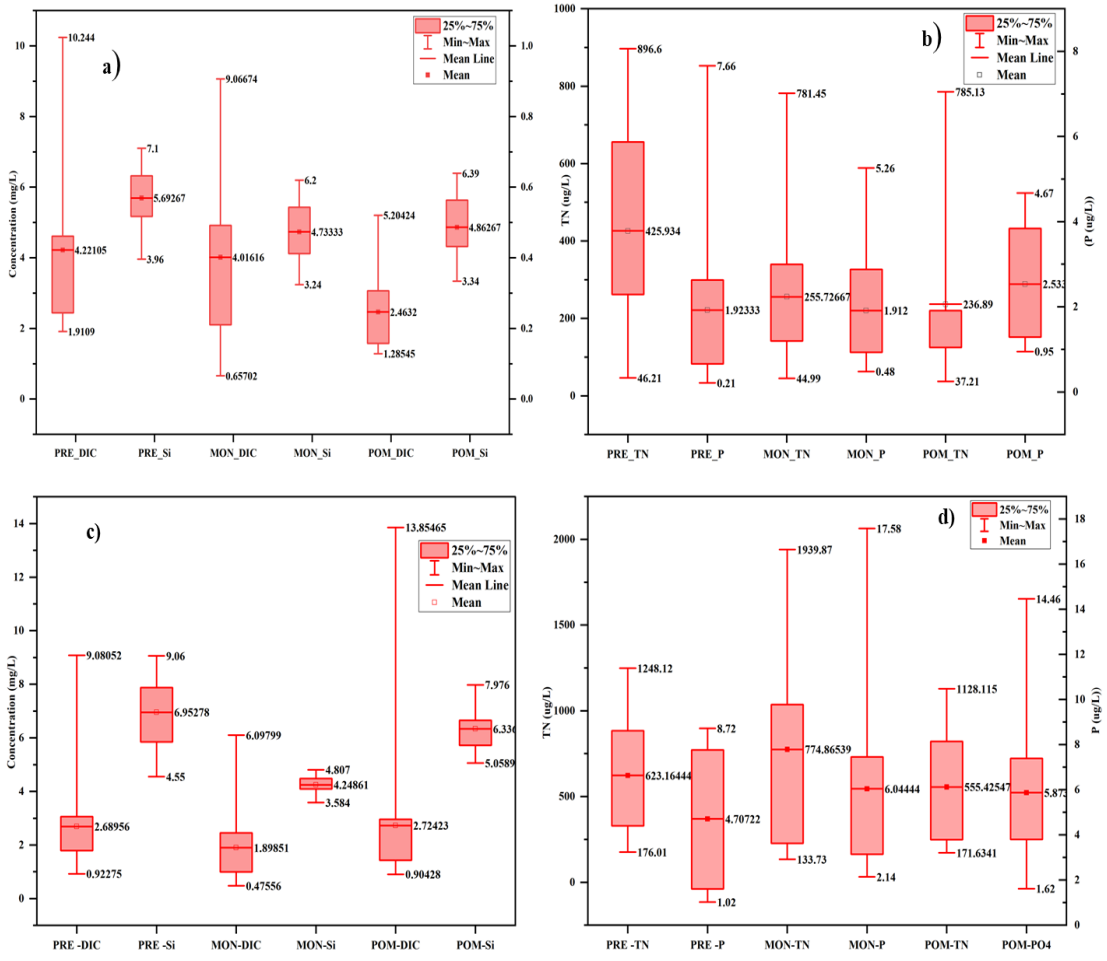

261 **Fig. 5:** Box plot representing seasonal concentrations of HCO_3^- and DSi in a) KRB, c) VRB and
262 DIN and DIP in b) KRB and d) VRB basins.

263 **3.4 Nutrient Ratios**

264 DIN: DIP ratios in both basins are consistently higher than the Redfield ratio of 16:1 (Cleveland
265 et al., 2007), suggesting an excess of DIN relative to DIP. In KRB, downstream region (urban
266 lowland) exhibited the highest nutrient yield, while the upstream forested region acted as a nutrient
267 sink with minimal export. The DSi:DIN ratios in both basins are considerably greater than 1 in the

https://doi.org/10.5194/egusphere-2026-995
Preprint. Discussion started: 6 March 2026

upstream regions, indicating an abundance of DSi over DIN. Moving downstream, the ratio decreases sharply, suggesting an enrichment of DIN irrespective of the season. In the KRB, the DSi:DIN ratio in the tributaries ranges between 4 and 11, showing relatively higher values during the POM and PRM seasons, while the lowest values occur during the MON period.

In the VRB, midstream region (plantation and agricultural areas) showed the highest nutrient load, while upstream region (low-gradient areas with small townships and agriculture) had the highest nutrient yield (Table 1). The DSi:DIN ratio exceeds 1 only in the upstream areas, while in the midstream and downstream regions, the values range approximately between 3 and 5. This pattern indicates a relatively balanced contribution of dissolved nitrate and silica as reported earlier (Nishitha et al., 2021). Similar to KRB, for the tributaries of VRB, the ratio remains higher during the PRM and POM seasons but drops during the monsoon.

The calculated N-ICEP and P-ICEP indices for both basins exhibit negative values, reflecting an overall excess of DSi relative to DIN and DIP. Among these, DIP concentrations remain comparatively lower, reinforcing its role as the primary limiting agent. The mean N-ICEP and P-ICEP values for KRB were -0.08 and -0.09 kg km^{-2} d^{-1}, while for VRB they were -0.03 and -0.05 kg km^{-2} d^{-1}, respectively, at the river outlets. When compared with global and Indian river systems, the ICEP values of both these tropical small mountainous rivers remain consistently negative, signifying a low eutrophication potential. Overall, the ICEP values calculated for both the KRB and VRB clearly indicate that DIP acts as the limiting nutrient. This suggests that the nutrient stoichiometry within these basins favors DSi enrichment over DIN and DIP.

https://doi.org/10.5194/egusphere-2026-995
Preprint. Discussion started: 6 March 2026

4. Discussion

4.1 Hydrological Controls of Nutrient Distribution

The spatiotemporal distribution of nutrients in the KRB and VRB is fundamentally controlled by monsoon-driven hydrological variability, which regulates the balance between dilution, catchment-scale solute mobilization, groundwater contributions, and in-stream biogeochemical processing (Fig. S4; Gurumurthy et al., 2012; Reddy et al., 2024; Upendra et al., 2025). During the PRM, reduced discharge enhances water residence time and increases the proportional influence of groundwater, promoting the accumulation of HCO_3^-, DIN, and DSi through intensified soil CO_2 fluxes, microbial mineralization, and prolonged water-rock interaction under baseflow-dominated conditions (Raj et al., 2023; Wen et al., 2024). In the upstream region, intense rainfall (~15000 mm; Reddy et al., 2019) during the MON season generates rapid hillslope runoff thus elevates erosional and leaching fluxes that mobilize both DIN and particulate-bound DIP from soils and anthropogenic sources (Ramos et al., 2019; Reddy et al., 2024). However, MON discharge simultaneously imposes strong dilution, selectively suppressing conservative weathering-derived solutes such as DIP and DSi, while amplifying source-driven constituents like DIN in agricultural and anthropogenic domestic sewage influenced tributaries of VRB. The contrasting physiography of the two basins further modulates these hydrological responses VRB's wider valleys and deeper regolith enhance nutrient retention and solute exchange during rising and falling limbs of the hydrograph, whereas KRB's steeper slopes and urbanized surface promote hydrological flashiness and rapid nutrient export, particularly limiting DIP accumulation despite high anthropogenic loading. Further, during the POM, mostly low-flow conditions, due to less rainfall, reinstating elevated HCO_3^- and DSi concentrations through reactivated weathering inputs and reduced dilution, while DIN and DIP reflect a combination of residual monsoon flushing,

https://doi.org/10.5194/egusphere-2026-995
Preprint. Discussion started: 6 March 2026

biological uptake, and internal cycling (Liu et al., 2020). The consistent downstream enrichment of DSi and DIN across seasons indicates cumulative solute loading governed by increasing drainage area, intensified sediment-water interactions, and enhanced mineral dissolution in lower reaches (Zhang et al., 2020; Reddy et al., 2024).

4.2 Segment-wise Processes Influencing Nutrient Dynamics

Segment-wise analysis of the KRB and VRB demonstrates that nutrient dynamics are governed by distinct hydrological and biogeochemical controls across the mountainous-midland-lowland continuum. In the upstream region, steep topography, dense forest cover, and rapid runoff maintain uniformly low nutrient levels, while intense silicate weathering and sustained groundwater inputs during the PRM season elevate both HCO_3^- and DSi, producing consistently high DSi:DIN ratios characteristic of WG catchments (Nishitha et al., 2021; Reddy et al., 2024). In midstream region, where agriculture, plantations, and rural settlements intensify, diversified flow pathways and enhanced soil disturbance increase nutrient delivery; DIN responds strongly to fertilizer mobilization and lateral subsurface transport during the MON season, while DIP rises moderately due to erosional inputs and active sediment water exchange, restricted to upstream region. This midstream zone functions as a key biogeochemical reactor where nitrification, mineral weathering, and sorption-desorption processes imprint pronounced seasonal variability. On the other hand, downstream region exhibits the clearest anthropogenic signature, with elevated DIN and DSi arising from sewage inputs (Nishitha et al., 2021), industrial discharge (Upendra et al., 2025), and intense chemical weathering (Upendra et al., 2025) in KRB, whereas in VRB, agrarian dominance and higher runoff retention enhance DIN exports and sustain greater background concentrations despite lower urbanization (Fig. S2). Increasing DIN and DSi concentrations toward the outlet in both basins arise through contrasting mechanisms rapid urban flushing in KRB versus sediment-

https://doi.org/10.5194/egusphere-2026-995
Preprint. Discussion started: 6 March 2026

mediated retention and release in VRB while tributaries modulate these patterns by reflecting localized land-use pressures, from industrial hotspots (KRB) to agricultural sub-basins (VRB). Collectively, the segment-wise patterns show that geomorphic gradients, land-use intensity, and monsoon-driven hydrological variability jointly control nutrient transformation and export, reinforcing silica-rich conditions and persistent phosphorus limitation across both tropical small mountainous river systems.

4.3 Controls on P-limitation and Si-rich Conditions

The plot of DIN: DSi ratios, using data from all seasons in both the KRB and VRB river basins, shows that most of the samples fall in the DIP limited region (Fig. 6). This indicates that DIP is the primary nutrient limiting biological productivity in both rivers (Fig. 6). This excess DIN may be attributed to agricultural runoff, sewage discharge, and other human activities, particularly in the mid and downstream segments, as specified earlier. DIP concentrations remain relatively low, possibly due to rapid uptake by plants and algae or binding to soil minerals, which is common in the acidic soils of tropical regions (Nishitha et al., 2021; Upendra et al., 2025). Recently, Reddy et al. (2021) attributed the dominance of autochthons source of particulate organic carbon further supporting the claim of in-situ production in these tropical small-scale mountainous rivers. Since long, the WG region has recognised as intense chemical weathering zone (Gurumurthy et al., 2012; Nishitha et al., 2021; Upendra et al., 2025). Thus, the higher DSi concentration in the current study further validates that the intense chemical weathering of silicate-rich rocks, such as gneiss and laterites, in the WG, particularly intensified during the MON season. In contrast, DIP remains persistently low (<10 $\mu g\ L^{-1}$; Fig. 4) due to strong sorption to organic and suspended matter (Reddy et al., 2024). Anthropogenic inputs disproportionately elevate DIN relative to DIP (Pandey et al., 2016), with sewage and urban stormwater dominating in KRB and fertilizer leaching and runoff

https://doi.org/10.5194/egusphere-2026-995
Preprint. Discussion started: 6 March 2026

retention driving DIN enrichment in VRB (Fig. 4). This imbalance consistently produces high DIN: DIP ratios and negative ICEP values, confirming P-limitation despite spatial variability in land use (Fig. 6). Seasonal and spatial patterns suggest that the hydrological transitions further strengthen these patterns, weathering-dominated headwaters supply abundant DSi and retain DIP, midstream mixed-use areas generate DIN through nitrification and fertilizer mobilization, and lowland reaches accumulate DIN through longer residence time and concentrated anthropogenic inputs. Overall, the stagnant conditions in the downstream region favors for high in-situ production that further supports the claim of limited DIP conditions in these small-west flowing coastal rivers (Fig. 6).

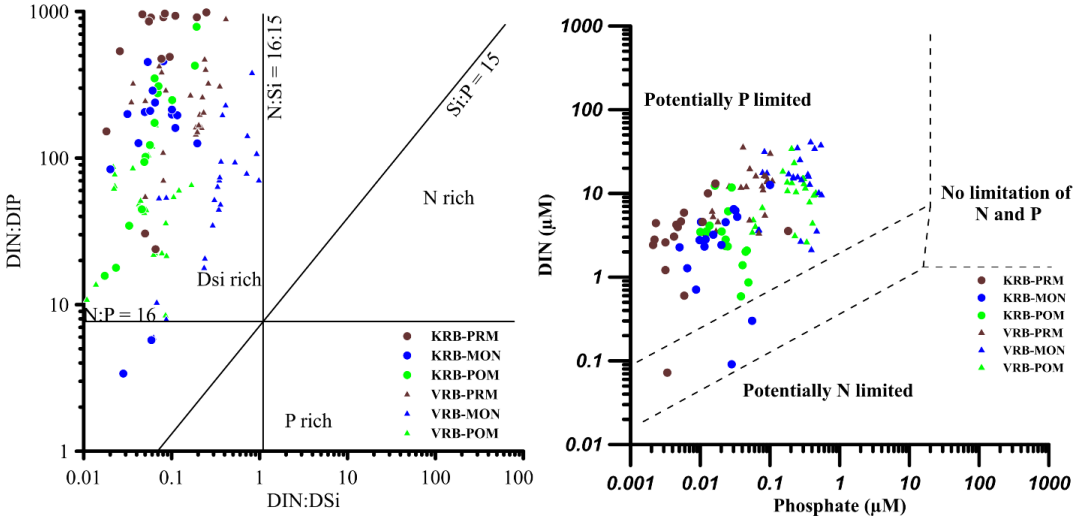

Fig. 6: Seasonal distribution of nutrient ratios in KRB and VRB basins.

4.4 Ecological Consequences

The pronounced P-limitation and Si-rich character of the KRB and VRB exert strong control over primary productivity, phytoplankton community structure, and downstream biogeochemical functioning (Peng et al., 2025). Persistent P scarcity suppresses diatom growth despite the high availability of DSi, leading to inefficient silica utilization and the downstream export of unused

https://doi.org/10.5194/egusphere-2026-995
Preprint. Discussion started: 6 March 2026

DSi to coastal waters (Chen et al., 2014). This imbalance limits the development of silica-requiring taxa and favours non-siliceous phytoplankton groups (e.g., cyanobacteria and chlorophytes) that can exploit elevated DIN while tolerating low DIP, potentially altering trophic pathways and reducing the nutritional quality of primary producers for higher consumers (Chu et al., 2014). High DIN: DIP ratios, particularly during PRM and POM when point-source inputs dominate, enhance the risk of N-fueled blooms of non-diatom species, even though overall eutrophication potential remains low due to negative ICEP values. It is also known that P-limitation within river channels constrains heterotrophic and autotrophic nutrient processing, reducing assimilation efficiency and allowing DIN to be exported downstream with minimal transformation (Peng et al., 2025). Similarly, the diatom production is suppressed under DIP scarcity (Srivastava et al., 2016; Lobo et al., 2016), biological uptake of DSi remains low, allowing DSi to accumulate downstream and in tributaries (Viaroli et al., 2013). This imbalance drives a pronounced decoupling of nutrient cycles, wherein nitrogen is efficiently mobilised through the fluvial network while DIP remains predominantly particle-associated and sediment-bound, weakening benthic–pelagic coupling and diminishing internal biogeochemical feedback that ordinarily regulates nutrient retention (Chen et al., 2014; Peng et al., 2025). Overall, it needs to be examined that the nutrient stoichiometry of the KRB and VRB reflects a watershed regime in which P-limitation restricts balanced primary productivity, weak biological DSi drawdown leads to Si accumulation, and sustained DIN availability promotes ecological shifts toward non-siliceous phytoplankton, collectively restructuring productivity, community composition, and biogeochemical coupling from headwaters to the coastal interface (Fig. 7). In addition to this, there are no reported evidences of overgrowth of phytoplankton or the presence of harmful algal blooms in the WG coast, particularly

https://doi.org/10.5194/egusphere-2026-995
Preprint. Discussion started: 6 March 2026

near the outlet region of KRB and VRB further confirms the less role of these nutrient inputs in the receiving coast ecosystem dynamics.

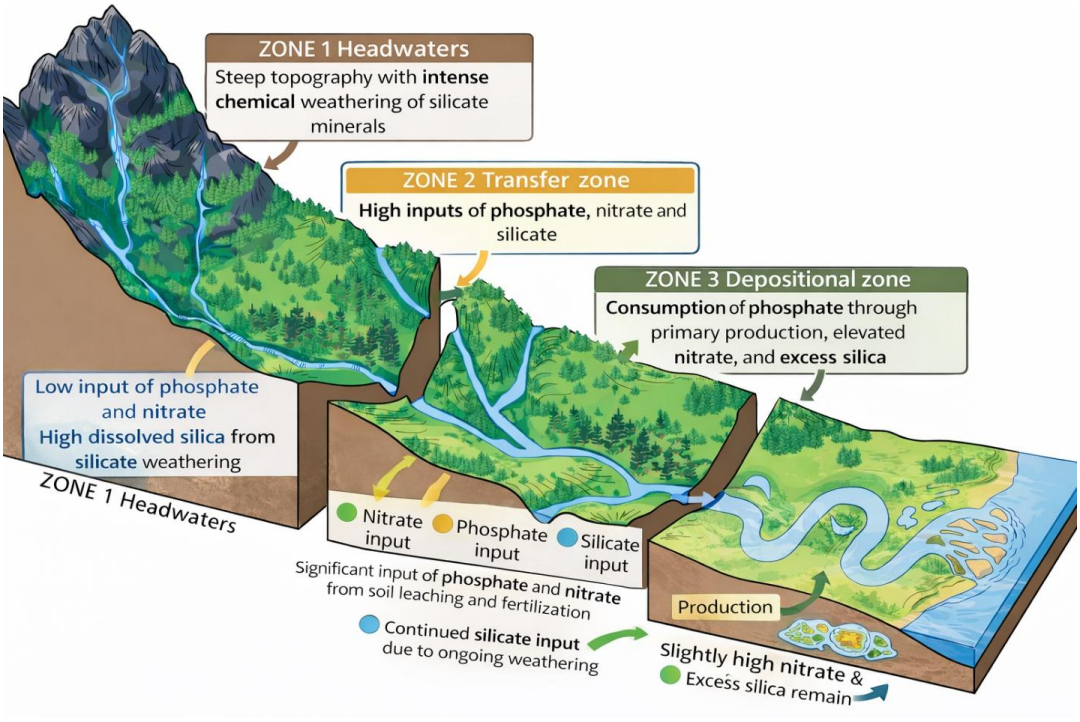

Fig. 7: Geomorphic control on nutrient and silica dynamics along the river continuum.

The conceptual model illustrates longitudinal hydrogeochemical evolution from headwaters to depositional lowlands. In the steep headwater zone (Zone 1), intense silicate mineral weathering under high-relief conditions generates elevated dissolved silica flux, while rapid runoff and short residence time limit phosphate and nitrate accumulation. In the transfer zone (Zone 2), increased tributary inflow and soil–water interaction enhances inputs of phosphate and nitrate, with continued downstream transport of weathering-derived silica. In the low-gradient depositional zone (Zone 3), prolonged water residence and floodplain stagnation promote primary production, resulting in preferential phosphate consumption, slightly elevated residual nitrate, and persistence

https://doi.org/10.5194/egusphere-2026-995
Preprint. Discussion started: 6 March 2026

of excess dissolved silica. The figure emphasizes the coupling between geomorphology, chemical weathering intensity, and nutrient utilisation along the river continuum.

5. Conclusion

A comprehensive assessment of common hydrochemistry and nutrient fluxes in the small tropical rivers, KRB and VRB, are studied in this study. The study concludes that the most of water sample of both river basin shows characteristics behaviour of Ca-Mg-HCO3 followed by Na-K-Cl-SO4, signify the water-rock interaction as main source for major ions in both the basins. The major focus study is assessing the nutrient fluxes, their distribution throughout the system and highlights the distinct biogeochemical characteristics of these tropical small catchments. The segment wise flux estimation shows that the higher contribution of DIN and DSi for both the river basin is coming from the downward region signifying the role of anthropogenic activities. The markedly high DSi flux of KRB, comparable to large global river systems such as the Amazon and Mississippi, further support the claim of intense silicate weathering in the tropical region due to interplay of lithology, intense monsoonal rainfall, and steep terrain. Similarly, the elevated HCO_3^- flux in KRB reflects active silicate weathering processes and substantial organic carbon input. In contrast, the VRB exhibits relatively higher DIP and DIN fluxes, suggesting stronger anthropogenic influences and nutrient mobilization through land use practices. This study finally stresses that both the rivers exhibiting P-limit systems due to in-situ production in the downstream region favoured by stagnant conditions. Overall, the study confirms the less influence of nutrient export dynamics in the receiving coastal ecosystem health with implications for high downstream productivity. Subsequent studies could explore seasonal and interannual changes in nutrient fluxes in small tropical rivers, integrating detailed land-use mapping, sediment dynamics, and modeling

https://doi.org/10.5194/egusphere-2026-995
Preprint. Discussion started: 6 March 2026

approaches, to clarify how topography, climate, and human activities collectively influence nutrient transport to downstream coastal ecosystems.

Acknowledgements

The authors wish to record their appreciation for the institutional backing and motivation provided by the Director of the National Centre for Earth Science Studies (NCESS) and the Head of the Environmental Hydrology Group (EHG). They also acknowledge the contributions of the EHG research staffs and technical personnel, whose support in laboratory operations and analytical procedures was essential to this work.

https://doi.org/10.5194/egusphere-2026-995
Preprint. Discussion started: 6 March 2026

Funding

The research presented in this manuscript was undertaken using internal funding support from the Ministry of Earth Sciences, Government of India. The authors confirm that no additional financial contributions were obtained from external organizations or funding bodies.

Declaration of Competing Interest

The authors state that no competing interests, financial or otherwise, exist in relation to this study.

Author's contribution statement

B. Upendra and S. Kiran Kumar Reddy: Conceptualized the study and wrote the original manuscript; **M. Ciba, K. Jesuraja, S. Vidya, P. Vinnetha:** Contributed to field sample collection laboratory analysis and data interpretation; **K. Anoop Krishnan**: Critically reviewed the manuscript and provided resources.

Data availability, Code availability, Code and data availability

The data presented in this article are available from the corresponding author upon reasonable request.

https://doi.org/10.5194/egusphere-2026-995
Preprint. Discussion started: 6 March 2026

Table 1: Region-wise nutrient flux estimation of KRB and VRB basins.

	Q ($km^3\ yr^{-1}$)	L_n ($t\ yr^{-1}$)				Y_n ($kg\ ha^{-1}yr^{-1}$)			
Segment	**Discharge**	**HCO_3^-**	**N**	**P**	**Si**	**HCO_3^-**	**N**	**P**	**Si**
KRB									
Upstream	0.46	694.74	32.40	0.35	1812.43	37.81	1.76	0.02	98.64
Midstream	1.47	1298.30	112.46	1.01	2241.61	76.17	6.08	0.03	121.16
Downstream	2.75	1786.96	119.85	0.44	1530.31	189.10	12.68	0.05	161.94
Total	**4.68**								
Average						**101.03**	**6.84**	**0.05**	**127.25**
VRB									
Upstream	0.58	194.98	39.64	0.99	894.59	14.13	2.87	0.04	64.83
Midstream	1.75	1116.14	442.84	4.09	2998.90	26.89	10.67	0.08	72.26
Downstream	2.07	130.81	23.66	0.30	124.64	81.75	14.78	0.11	107.90
Total	**4.40**								
Average						**40.92**	**9.44**	**0.07**	**81.66**

https://doi.org/10.5194/egusphere-2026-995
Preprint. Discussion started: 6 March 2026

References

1. Ahmed, M. (2008). Geochemical and isotopic characteristics of Quaternary aquifer in Sohag District, Upper Egypt. Arab J Nucl Sci Appl, 41(1), 129-146.

2. Aju, C.D., Reghunath, R., Achu, A.L. et al. Understanding the hydrogeochemical processes and physical parameters controlling the groundwater chemistry of a tropical river basin, South India. Environ Sci Pollut Res 29, 23561–23577 (2022). https://doi.org/10.1007/s11356-021-17455-w.

3. Alexander, R. B., Smith, R. A., Schwarz, G. E., Boyer, E. W., Nolan, J. V., & Brakebill, J. W. (2008). Differences in phosphorus and nitrogen delivery to the Gulf of Mexico from the Mississippi River Basin. Environmental science & technology, 42(3), 822-830.

4. Aniebone, V. O., Imo, D. O., & Shonde, O. O. (2024). Nutrients Pollution of the Coastal Marine Ecosystems. International Journal of Innovative Agriculture & Biology Research, 12(2), 82-95.

5. Anu-Sha, A. P., Baiju, K. R., & Justine, K. A. (2024). Geochemistry of granulitic rocks from the western Madurai Block, Southern Granulite Terrain, India and its Madagascar linkage. Journal of Mineralogical and Petrological Sciences, 119(1), 221212.

6. Badimela, U., Manohar, C., Kamaraj, J., James, A., Upasana, A., Ganugapenta, S., & Krishnan, A. (2024). Dynamic analysis of soil erosion and sediment yield engrossment involving rainfall, land use and land cover impacts using GIS-based RUSLE & SDR modeling: southern western Ghats River Basin of Kerala, India. Geosciences Journal, 28(6), 959-980.

7. Basu, N. B., Destouni, G., Jawitz, J. W., Thompson, S. E., Loukinova, N. V., Darracq, A., ... & Rao, P. S. C. (2010). Nutrient loads exported from managed catchments reveal emergent biogeochemical stationarity. Geophysical Research Letters, 37(23).

8. Billen, G., & Garnier, J. (2007). River basin nutrient delivery to the coastal sea: assessing its potential to sustain new production of non-siliceous algae. Marine Chemistry, 106(1-2), 148-160.

9. Bouwman, A. F., Beusen, A. H., & Billen, G. (2009). Human alteration of the global nitrogen and phosphorus soil balances for the period 1970–2050. Global biogeochemical cycles, 23(4).

10. Chadha, D. K. (1999). A proposed new diagram for geochemical classification of natural waters and interpretation of chemical data. Hydrogeology journal, 7, 431-439.

https://doi.org/10.5194/egusphere-2026-995
Preprint. Discussion started: 6 March 2026

11. Cleveland, C.C., Liptzin, D. (2007). C:N:P stoichiometry in soil: is there a "Redfield ratio" for the microbial biomass?. Biogeochemistry 85, 235–252 https://doi.org/10.1007/s10533-007-9132-0.

12. Conley, D. J., Paerl, H. W., Howarth, R. W., Boesch, D. F., Seitzinger, S. P., Havens, K. E., ... & Likens, G. E. (2009). Controlling eutrophication: nitrogen and phosphorus. Science, 323(5917), 1014-1015.

13. David, S. E., Chattopadhyay, M., Chattopadhyay, S., & Jennerjahn, T. C. (2016). Impact of human interventions on nutrient biogeochemistry in the Pamba River, Kerala, India. Science of the Total Environment, 541, 1420-1430.

14. Finkler, N. R., Gücker, B., & Cunha, D. G. F. (2023). Nutrient uptake in tropical rivers receiving wastewater treatment plant discharge: high mass removal but low nutrient uptake efficiencies. *Ecological Indicators*, *154*, 110865.

15. Fu, M., Wang, Z., Pu, X., Xu, Z., & Zhu, M. (2012). Changes of nutrient concentrations and N: P: Si ratios and their possible impacts on the Huanghai Sea ecosystem. Acta Oceanologica Sinica, 31, 101-112.

16. Garnier, J., Beusen, A., Thieu, V., Billen, G., & Bouwman, L. (2010). N: P: Si nutrient export ratios and ecological consequences in coastal seas evaluated by the ICEP approach. Global Biogeochemical Cycles, 24(4).

17. Guo L., Zhang J. Z. & Gueguen C. (2004). Speciation and fluxes of nutrients (N, P, Si) from the upper Yukon River. Global Biogeochemical Cycles 18, GB1038. 12 PP.

18. Gupta, H., Reddy, K. K., Gandla, V., Paridula, L., Chiluka, M., & Vashisth, B. (2022). Freshwater discharge from the large and coastal peninsular rivers of India: a reassessment for sustainable water management. Environmental Science and Pollution Research, 29(10), 14400-14417.

19. Houser, J. N., & Richardson, W. B. (2010). Nitrogen and phosphorus in the Upper Mississippi River: transport, processing, and effects on the river ecosystem. Hydrobiologia, 640(1), 71-88.

20. Krishna, M. S., Viswanadham, R., Prasad, M. H., Kumari, V. R., & Sarma, V. V. (2019). Export fluxes of dissolved inorganic carbon to the northern Indian Ocean from the Indian monsoonal rivers. Biogeosciences, 16(2), 505-519.

https://doi.org/10.5194/egusphere-2026-995
Preprint. Discussion started: 6 March 2026

21. Li, M., Xu, K., Watanabe, M., & Chen, Z. (2007). Long-term variations in dissolved silicate, nitrogen, and phosphorus flux from the Yangtze River into the East China Sea and impacts on estuarine ecosystem. Estuarine, Coastal and Shelf Science, 71(1-2), 3-12.

22. Li, R. H., Liu, S. M., Li, Y. W., Zhang, G. L., Ren, J. L., & Zhang, J. (2014). Nutrient dynamics in tropical rivers, lagoons, and coastal ecosystems of eastern Hainan Island, South China Sea. Biogeosciences, 11(2), 481-506.

23. Lobo, E. A., Heinrich, C. G., Schuch, M., Wetzel, C. E., & Ector, L. (2016). Diatoms as bioindicators in rivers. In *River algae* (pp. 245-271). Cham: Springer International Publishing.

24. Meybeck, M. (1982). Carbon, nitrogen, and phosphorus transport by world rivers. American journal of Science, 282(4), 401-450.

25. Mukherjee, M., Suresh, V. R., & Manna, R. K. (2018). Microplankton dynamics of a coastal lagoon, Chilika: interactive effect of environmental parameters on microplankton groups. Environmental monitoring and assessment, 190(11), 689.

26. Mulholland, P. J., Helton, A. M., Poole, G. C., Hall, R. O., Hamilton, S. K., Peterson, B. J., ... & Thomas, S. M. (2008). Stream denitrification across biomes and its response to anthropogenic nitrate loading. Nature, 452(7184), 202-205.

27. Nie, J., Feng, H., Witherell, B. B., Alebus, M., Mahajan, M. D., Zhang, W., & Yu, L. (2018). Causes, assessment, and treatment of nutrient (N and P) pollution in rivers, estuaries, and coastal waters. Current pollution reports, 4(2), 154-161.

28. Padmalal, D. (1996). Sedimentary structures and texture of the Warkalli sandstone (Mio-Pliocene) at Cherunniyoor, Kerala. Journal Geological Society of India, 48(4), 403-407.

29. Rangel-Buitrago, N., Galgani, F., & Neal, W. J. (2024). Addressing the global challenge of coastal sewage pollution. Marine Pollution Bulletin, 201, 116232.

30. Ravi, N. K., Srivastava, A., Ram, K., & Jha, P. K. (2021). Nutrient chemistry and eutrophication risk assessment of the Ghaghara river, India. Water Supply, 21(7), 3486-3502.

31. Reddy, S. K. K., Gupta, H., & Reddy, D. V. (2019). Dissolved inorganic carbon export by mountainous tropical rivers of the Western Ghats, India. Chemical Geology, 530, 119316.

32. Reddy, S. K. K., Gupta, H., Gandla, V. K., Reddy, D. V., Kurakalva, R. M., & Kumar, D. (2024). Nutrient dynamics in small west-flowing tropical mountainous rivers of India. Applied Geochemistry, 169, 106035.

https://doi.org/10.5194/egusphere-2026-995
Preprint. Discussion started: 6 March 2026

575 33. Reddy, S. K. K., Gupta, H., Badimela, U., Reddy, D. V., Kurakalva, R. M., & Kumar, D.
576 (2021). Export of particulate organic carbon by the mountainous tropical rivers of Western Ghats,
577 India: Variations and controls. Science of the Total Environment, 751, 142115.
578 34. Seitzinger, S. P., Harrison, J. A., Dumont, E., Beusen, A. H., & Bouwman, A. F. (2005).
579 Sources and delivery of carbon, nitrogen, and phosphorus to the coastal zone: An overview of
580 Global Nutrient Export from Watersheds (NEWS) models and their application. Global
581 biogeochemical cycles, 19(4).
582 35. Srivastava, P., Verma, J., Grover, S., & Sardar, A. (2016). On the importance of diatoms as
583 ecological indicators in river ecosystems: A review. *Indian J Plant Sci*, *5*(1), 70-86.
584 36. Stosch, H.-G. (2022). Excel template to plot hydrochemical data into a Piper diagram (1.0).
585 Zenodo. https://doi.org/10.5281/zenodo.5994293.
586 37. Sunil, P. S., Radhakrishna, M., Kurian, P. J., Murty, B. V. S., Subrahmanyam, C., Nambiar,
587 C. G., ... & Mohan, S. K. (2010). Crustal structure of the western part of the Southern Granulite
588 Terrain of Indian Peninsular Shield derived from gravity data. Journal of Asian Earth Sciences,
589 39(6), 551-564.
590 38. Tong, Y., Zhao, Y., Zhen, G., Chi, J., Liu, X., Lu, Y., Wang, X., Yao, R., Chen, J. and Zhang,
591 W. (2015). Nutrient loads flowing into coastal waters from the main rivers of China (2006–2012).
592 Scientific reports, 5(1), p.16678.
593 39. Turner, R. E., Rabalais, N. N., Justic', D., & Dortch, Q. (2003). Global patterns of dissolved
594 N, P and Si in large rivers. Biogeochemistry, 64(3), 297-317.
595 40. Tyagi, S., Dobhal, R., Kimothi, P.C. et al. Studies of River Water Quality Using River Bank
596 Filtration in Uttarakhand, India. Water Qual Expo Health 5, 139–148 (2013).
597 https://doi.org/10.1007/s12403-013-0097-z.
598 41. Upendra, B., Ciba, M., Rahul, S., Sreenivasulu, G., Reddy, S. K. K., Arun, V., & Krishnan,
599 K. A. (2025). Dissolved load, chemical weathering, and CO2 uptake dynamics of small tropical
600 mountainous rivers of Southern Granulite Terrain, Karamana and Vamanpuram, Western Ghats,
601 India. Scientific Reports, 15(1), 11684.
602 42. Varghese, T. I., Prakash, T. N., & Nagendra, R. (2016). Depositional history of coastal plain
603 sediments, Southern Kerala, South West India. Journal of Earth Science and Climatic Change,
604 7(355), 1-8.

https://doi.org/10.5194/egusphere-2026-995
Preprint. Discussion started: 6 March 2026

605 43. Varma, K., & Jha, P. K. (2023). Spatial and seasonal variations in nutrient load and trophic
606 status of Ganga and Yamuna rivers in Uttar Pradesh, India. Water Supply, 23(6), 2553-2574.
607 44. Varma, K., & Jha, P. K. (2023). Spatial and seasonal variations in nutrient load and trophic
608 status of Ganga and Yamuna rivers in Uttar Pradesh, India. Water Supply, 23(6), 2553-2574.
609 45. Varma, K., & Jha, P. K. (2024). Phosphorus distribution in the water and sediments of the
610 Ganga and Yamuna Rivers, Uttar Pradesh, India: Insights into pollution sources, bioavailability,
611 and eutrophication implications. Environmental Monitoring and Assessment, 196(4), 336.
612 46. Viaroli, P., Nizzoli, D., Pinardi, M., Rossetti, G., & Bartoli, M. (2013). Factors affecting
613 dissolved silica concentrations, and DSi and DIN stoichiometry in a human impacted watershed
614 (Po River, Italy). Silicon, 5, 101-114.
615 47. Wei, Z., Yu, Y., & Yi, Y. (2023). Analysis of future nitrogen and phosphorus loading in
616 watershed and the risk of lake blooms under the influence of complex factors: Implications for
617 management. Journal of Environmental Management, 345, 118662.
618 48. Wollheim, W. M., Peterson, B. J., Thomas, S. M., Hopkinson, C. H., & Vörösmarty, C. J.
619 (2008). Dynamics of N removal over annual time periods in a suburban river network. Journal of
620 Geophysical Research: Biogeosciences, 113(G3).
621 49. Zeng, Z., Chen, F., Lao, Q., & Zhu, Q. (2025). Effects of Nutrients on the Phytoplankton
622 Community Structure in Zhanjiang Bay. Journal of Marine Science and Engineering, 13(7), 1202.
623 50. Zhang, P., Xu, J. L., Zhang, J. B., Li, J. X., Zhang, Y. C., Li, Y., & Luo, X. Q. (2020).
624 Spatiotemporal dissolved silicate variation, sources, and behavior in the eutrophic Zhanjiang Bay,
625 China. Water, 12(12), 3586.